Iran. J. Biotechnol. July 2023;21(3): e3505 DOI: 10.30498/ijb.2023.362229.3505

Research Article

The Effect of Collagen and Fibrin Hydrogels Encapsulated with Adipose Tissue Mesenchymal Stem Cell-Derived Exosomes for Treatment of Spinal Cord Injury in a Rat Model

Zohreh Afsartala[1], Mahmoudreza Hadjighassem[1], Sadegh Shirian[2,3], Somayeh Ebrahimi-Barough[4], Leila Gholami[5], Gilda Parsamanesh[6], Ziba Veisimalekshahi[7], Latifeh Karimzadehbardeei[8], Jafar Ai[1*]

[1]Brain and Spinal Cord Injury Research Center, Neuroscience Institute, Tehran University of Medical Science, Tehran, Iran
[2]Department of Pathology, School of Veterinary Medicine, Shahrekord University, Shahrekord, Iran
[3]Shiraz Molecular Pathology Research Center, Dr. Daneshbod Pathology Lab, Shiraz, Iran
[4]Department of Tissue Engineering and Applied Cell Sciences, School of Advanced Technologies in Medicine, Tehran University of Medical Sciences, Tehran, Iran
[5]Department of Periodontics, Dental Research Center, School of Dentistry, Hamadan University of Medical Sciences, Hamadan, Iran
[6]Department of Immunology, School of Medicine, Tehran University of Medical Sciences, Tehran, Iran
[7]Department of Medical Biotechnology School of Advanced Technologies in Medical, Tehran University of Medical Sciences
[8]Department of Animal Biology, School of Biology, College of Science, University of Tehran, Tehran, Iran

[*]*Corresponding author*: Jafar Ai, Brain and Spinal Cord Injury Research Center, Neuroscience Institute, Tehran University of Medical Science, Tehran, Iran. Tel:+98-2143052000, Fax:+98-88991117, E-mail: jafar_ai@tums.ac.ir

Received: 2022/09/15 ; **Accepted:** 2023/03/12

Background: Mesenchymal stem cell (MSC) derived exosomes (MSC-DE) have been demonstrated to be potential candidates for the treatment of rat spinal cord injury (SCI).

Objective: The effect of AD-MSC and AD-MSC-DE encapsulated into collagen and fibrin hydrogels on the treatment of SCI in a rat animal model was investigated for introducing a new effective SCI treatment method

Materials and Methods: The AD-MSC-DE was isolated using ultra-centrifugation at 100,000×g for 120 min and characterized by different methods. Fibrin and collagen hydrogels were synthesized and then mixed with AD-MSC-DE suspension. the characterized AD-MSC-DE were encapsulated into collagen and fibrin hydrogels. eighteen adult male Wister rats were randomly classified into 3 equal groups (n=6): the control group (SCI rat without treatment), SCI rat treated with either AD-MSC-DE encapsulated in collagen hydrogel or encapsulated in fibrin hydrogel groups. the treatment approaches were evaluated using clinical, histological, and molecular assays.

Results: The AD-MSC-DE encapsulated into fibrin and collagen groups showed better clinical function than the control group. The AD-MSC-DE encapsulated into fibrin and collagen also improved SCI-induced polio and leuko-myelomalacia and leads to higher expression of NF protein than the control group. In the AD-MSC-DE encapsulated into collagen and fibrin leads to up-regulation the mean levels of NEFL (23.82 and 24.33, respectively), eNOS (24.31 and 24.53, respectively), and CK19 mRNAs (24.23 and 23.98, respectively) compared to the control group.

Conclusion: The AD-MSC-DE encapsulated within ECM-based hydrogel scaffolds such as collagen and fibrin can regenerate the injured nerve in SCI rats and reduce spinal cord lesion-induced central neuropathic pain.

Keywords: Adipose Mesenchymal Stem Cell-Derived Exosomes, Collagen, Fibrin, Hydrogel, Spinal Cord Injury

1. Background

Acute traumatic SCI affects more than 27 million people in the world (1, 2). SCI leads to quadriplegia, paraplegia, and permanent or temporary changes in the cord's normal functions (3). SCI patients show serious motor and sensory impairments that result in a dramatic loss of life quality and depression (4). despite the clinically available therapies including hemodynamic therapy, invasive spinal cord pressure monitoring, corticosteroids, surgical decompression, and tissue engineering (5-10), effective functional recovery has yet to be introduced. The inhibitory microenvironment induced by severe oxidative stress, inflammation, damage of the extracellular matrix, and hypoxic ischemia is the main challenge for the effective treatment of SCI (2, 11). A complete regulation of the local inhibitory microenvironment has been suggested to be effective for SCI treatment (12).

Regenerative medicine and the transplantation of MSC, induced pluripotent SCs, and embryonic SCs have been previously shown to be effective in SCI treatment (13) by regulation of the SCI lesion microenvironment (14). However, the effective treatment of cell transplantation is widely limited due to the low survival rate of transplanted cells within the lesion area after stem cell transplantation (15, 16). The stem cells play a critical therapeutic role in the lesions such as SCI lesions by releasing factors into their surroundings through a paracrine mechanism, e.g. EVs. therefore, EVs such as exosomes have been recently introduced (17-19). Stem cells-derived EVs therapy provides a safe and reliable way to regenerate or replace the injured tissues (18, 19). MSC-Derived Exosomes (MSC-DE) also play an important mediatory role in Cell-Cell communication their therapeutic potential in SCI has attracted extensive attention in recent years. Local implantation of AD-MSC-DE has been demonstrated to be a promising therapeutic approach in SCI (4). Three-dimensional biocompatible scaffolds, especially hydrogels, are suggested for tissue bridging, effective delivery of exosomes, angiogenesis, and neurogenesis (20). Therefore, the current study was designed to investigate the effect of collagen and fibrin hydrogel encapsulation of adipose tissue MSC-DE (AD-MSC-DE) for the treatment of SCI in a rat animal model.

2. Objectives

In this study, the regenerative effect of adipose tissue mesenchymal stem cells and their exosome derived encapsulated into collagen and fibrin hydrogel scaffolds in spinal cord injury in a rat animal model is evaluated for finding a new, effective, and applied method for treatment of SCI.

3. Materials and Methods

3.1. In Vitro Study

3.1.1. Isolation of Adipose Tissue Mesenchymal Stem Cells

Peri-epididymal adipose tissue was used for the isolation of the AD-MSC as previously described (21). The isolated adipose tissues were first dissolved in collagenase type I (2 mg. L^{-1}, Sigma-Aldrich) at room temperature (RT) for 1 hour and gently shacked. The collagenase was then neutralized using DMEM (Gibco, Germany) containing 10% fetal bovine serum (FBS) (Gibco, Germany) and penicillin/streptomycin (1%) and then filtered using 40- and 70-µm filters and finally was centrifuged at 1500 (x g) for 10 min. The culture media were replaced every four days and finally, the AD-MSC at passage 3 were characterized for CD73, and CD105 expression as well as the expression of the hematopoietic markers (CD34, CD45, and, CD11b) by using flow cytometry. The isolated cells were differentiated into osteogenic cells such as lipoblasts and osteoblasts and stained using specific staining of Oil-Red-O and Alizarin Red S, respectively.

3.1.2. Isolation of Adipose Tissue Mesenchymal Stem Cells Derived Exosomes

The exosomes were isolated using ultra-centrifugation. After reaching the AD-MSC to a confluency of 70%, cell supernatant was centrifuged at 2000× g and 10,000× g for 2h at 4 °C to remove cell debris and larger particles, respectively. To obtain the pellet cells containing exosomes, the supernatants were centrifuged using ultra-centrifugation at 100,000×g for 120 minutes at 4 °C and the pellet cells were washed twice with phosphate-buffered saline (PBS).

3.1.3. Determination of AD-MSC-DE Concentration

The concentration of AD-MSC-DE was determined using Bradford's assay. Briefly, various bovine serum albumin (BSA) concentrations were prepared and 10 µL of each concentration was placed in a 6-well plate. A total of 200 µL of Bradford's solution was

added to each well. The absorbance was determined at a wavelength of 595nm and the concentration of exosome at 1mL of BPS solution was determined using a standard curve (22).

3.1.4. Characterization of Exosome

3.1.4.1. Scanning Electron Microscopy

For fixation of the exosomes, the precipitated EVs were placed directly on the glass slides, and mixed with a volume of the 5% glutaraldehyde solution prepared in PBS. The slides were then dehydrated in a series of increasing ethanol concentrations (70, 80, and 95% ethanol solutions) and dried on air. A 5-µL drop of PBS was spread on the glass using all of the above-mentioned procedures for negative control. SEM (Zeiss Merlin with auto-emission cathode, Germany) was used to scan the surface of the specimen at a 200- to 400-V acceleration voltage and generate topographical information.

3.1.4.2. Dynamic Light Scattering

The isolated exosomes from the AD-MSC were diluted at a concentration of 0.1 $\mu g.\mu L^{-1}$ using Dulbecco's PBS (DPBS) and transferred into a disposable low-volume cuvette (UVette, Eppendorf Austria GmbH, Austria) that finally is filled up to 100 µL with DPBS. A W130i apparatus (Avid Nano Ltd., UK) was used to measure DLS. To confirm standardization and reproducibility, the parameter values were fixed as previously described by Liu *et al*. (2021) (23).

3.1.4.3. Western Blotting

The isolated AD-MSC-DEs were loaded on 10% SDS-polyacrylamide electrophoresis gel and then transferred into the membranes with Trans-Blot® Turbo™ Transfer Packs (Biorad, Hercules, USA) to separate the proteins. The 5% non-fat dry milk in PBS containing Tween 20 (0.1%) was applied to block the membranes. The blots were incubated overnight with CD63 primary antibody after blocking the membranes. The blocked membranes were washed twice in PBS containing Tween 20 (0.5%) and incubated with the secondary antibody (horseradish peroxidase (HRP)-conjugated goat anti-mouse antibody, Abcam, USA). The samples were finally washed and the proteins were visualized using the Amersham Biosciences ECL system. A Proxima 2850 Imager (IsoGen Life Sciences, The Netherlands) was used to obtain the images. Signal intensity was quantified using Image J software (1.8.0 version).

3.1.5. Fibrin and Collagen Hydrogels Synthesis

Collagen was extracted from the collagen fibers, which exist in rat tails as previously reported by Bakhtiarimoghadam *et al.* (2021) (15). In brief, 1g of the extracted collagen was dissolved in 1L acetic acid (0.001 M), and then 0.5 mL of the yielded collagen solution was poured into a 6-well plate and 100 µL of PBS (pH=7.4) and 200 µL of DMEM were added to each well. To prevent premature gelation, the plates were placed on ice, and for collagen hydrogel formation; the plates were incubated at RT for 30 min.

For the preparation of fibrin hydrogel, 1.5 mg of lyophilized bovine fibrinogen (Sigma Aldrich, MO) was dissolved in 0.5 mL of 199 M acetic acid solution (Sigma Aldrich, MO) and then transferred to a 6-well culture plate. The solution was enriched by adding 15µL of thrombin solution (126 U/2.4 mL in NaCl [1 M], Sigma-Aldrich), 200 µL of DMEM, and 100 µL of FBS and then incubated at 37 ºC for 3 h to create the clot. Both the prepared collagen and fibrin hydrogels were finally mixed with AD-MSC-DE suspension.

3.2. In Vivo Study

In this step of the study, 18 adults male Wistar rats, weighted 250–300 g, were provided according to the TUMS guidelines for animal care and use. The rats were obtained from a breeding colony and kept in individual cages in a standard condition cycle (12h lightness and 12h darkness) with free access to tap water and commercial food. The animals were then randomly divided into 3 groups of 6 rats each. The first group of the SCI contusion model was treated with AD-MSC-DE encapsulated in fibrin hydrogel and the other SCI contusion group was treated with AD-MSC-DE encapsulated in collagen hydrogel. the control group (SCI contusion rat model) received no treatment. To induce Sthe Lexington Precision Systems, Instrumentation was used following the weight compression method (24). Briefly, the animals were first anesthetized with an injection of ketamine (80 $mg.\ kg^{-1}$) and xylazine (10 $mg.\ kg^{-1}$), intra-peritoneally (IP) (25). After shaving the dorsal skin of the animal, the shaved area was disinfected by ethanol 70 % (v/v) and laminectomy was done at T9 and T10 (spinal T9-1levelsvel. The spinal cord was exposed by a midline

incision in the laminectomy area (7). The equal compression and pressure distribution on the exposed spinal cord was provided using a 35-g weight with a concave shape and area of 6.6 mm^2 for 15 minutes. The encapsulated AD-MSC-DE suspensions within both fibrin and collagen hydrogels were transplanted into the lesion area using a Hamilton syringe. The muscles and skin were then sutured. The rats received 1mL of lactated Ringer's solution, IP, for 5 days after treatment to hydrate the rats. Their urinary bladders were compressed manually twice daily for 2 weeks post-treatment. BBB locomotor scoring was used for clinical assessment of motor function at 1 and 3 days post-treatment and weekly for 4 weeks.

3.2.1. Thermal Escape Test

A hot plate-based thermal escape test was used for the evaluation of SCI-induced neuropathic pain at a temperature of 52 °C. In brief, the animals were located on an aluminum hot plate at 52 °C, and their thermal sensitivity was evaluated by toe parameters including foot-licking and jumping at days 1, 3, 5,7, 14, 21, and 28 post-treatment (26).

3.2.2. Microscopic Examination

On the 8th week post-treatment, the animals were sacrificed for Histopathological, Immunohistochemical, and Molecular analyses.

3.2.3. Histopathology

The treated spinal cord segments were resected, fixed in 10% formalin buffer (Merck, Germany), embedded in paraffin, cut at 4 to 5-µm thickness, and finally stained using routine hematoxylin and eosin method. An expert veterinarian pathologist blindly evaluated The histological tissue sections and reported.

3.2.4. Immunohistochemistry

The deparaffinized slide sections (3µM) w
are used for evaluating the expression of NF as previously described by Mahya *et al*. (2021) (7).

3.2.5. Molecular Assay

Finally, we have analyzed the mRNAs expression levels of NEFL, eNOS, and CK19 that are not normally expressed in SCI tissue.

3.2.5.1 RNA Extraction and cDNA Synthesis

The RiboEX RNA extraction kit (South Korea) was used to extract the total RNA based on the manufacturer's protocol. The isolated RNA with a 260/280 ratio of ~2 was chosen and reverse-transcribed to cDNA using the First Strand cDNA Synthesis Kit (ThermoScientific RevertAid).

The mRNA expression levels of NEFL, eNOS, and CK19 were determined by quantitative real-time PCR using SYBR green. GAPDH and ACTB were used as the internal comparator in parallel with the control sample. The primer sequences are shown in **Table 1** (**supplementary 1**). The primers were validated first for experiments. The PCR reaction mixture was prepared using 0.5 µL from each of the forward and reverse primers (10 p moL). Quantitative (q) Real-time PCR was done using a Rotor–Gene Q machine and mRNA expression levels were analyzed using StepOne software V2.0 (Fisher Scientific, UK), and the baseline and threshold were set manually. QRT-PCR data were analyzed using the ΔΔCt method.

Table. 1. The sequences (5′ to 3′ direction) of the used primers

ACTB	Forward: 5` GATCAAGATCATTGCTCCTCCTG 3` Reverse: 5` CTAGAAGCATTTGCGGTGGAC 3`
GAPDH	Forward: 5` TCGGAGTCAACGGATTTG 3` Reverse: 5` CCTGGAAGATGGTGATGG 3`
NEFL	Forward: 5` CGCCACCATGAGTTCCTTCA 3` Reverse: 5` GACTGGGCATCAACGATCCA 3`
eNOS	Forward: 5` GTTTGACCAGAGGACCCAGG 3` Reverse: 5` CCCGTCAGTTGGTAGGTTCC 3`
CK19	Forward: 5` GACACCATTCCTCCCTTCCC 3` Reverse: 5` CGACTGGCGATAGCTGTAGG 3`

3.3. Statistical Analysis

Data were analyzed using SPSS (version 22) and all data are expressed as the mean ± SEM. For analysis of the statistical differences among all experiment groups, One-way ANOVA was used and then followed by post hoc Tukey's test. The *p-values* less than 0.05 were considered statistically significant.

4. Results

4.1. Preparation of Stem Cells-Derived Exosomes

The characterized AD-MSC by specific surface markers for MSC were used for the isolation of exosomes (26). Subsequently, the exosomes isolated from AD-MSC were subjected to DLS, Western blotting, and scanning electron microscopy (SEM). The analyzed DLS and SEM images using Image J showed that the size of the exosomes, derived from the AD-MSC, was less than 100 nM (**Fig. 1A, 1B**).

4.2. Western Blotting

To detect proteins that are specifically expressed or not resident in the isolated exosomes Western blot analysis was used. The CD63 marker which is one of the well-known tetraspanins, was expressed to be enriched in the exosomes (**Fig. 1C**).

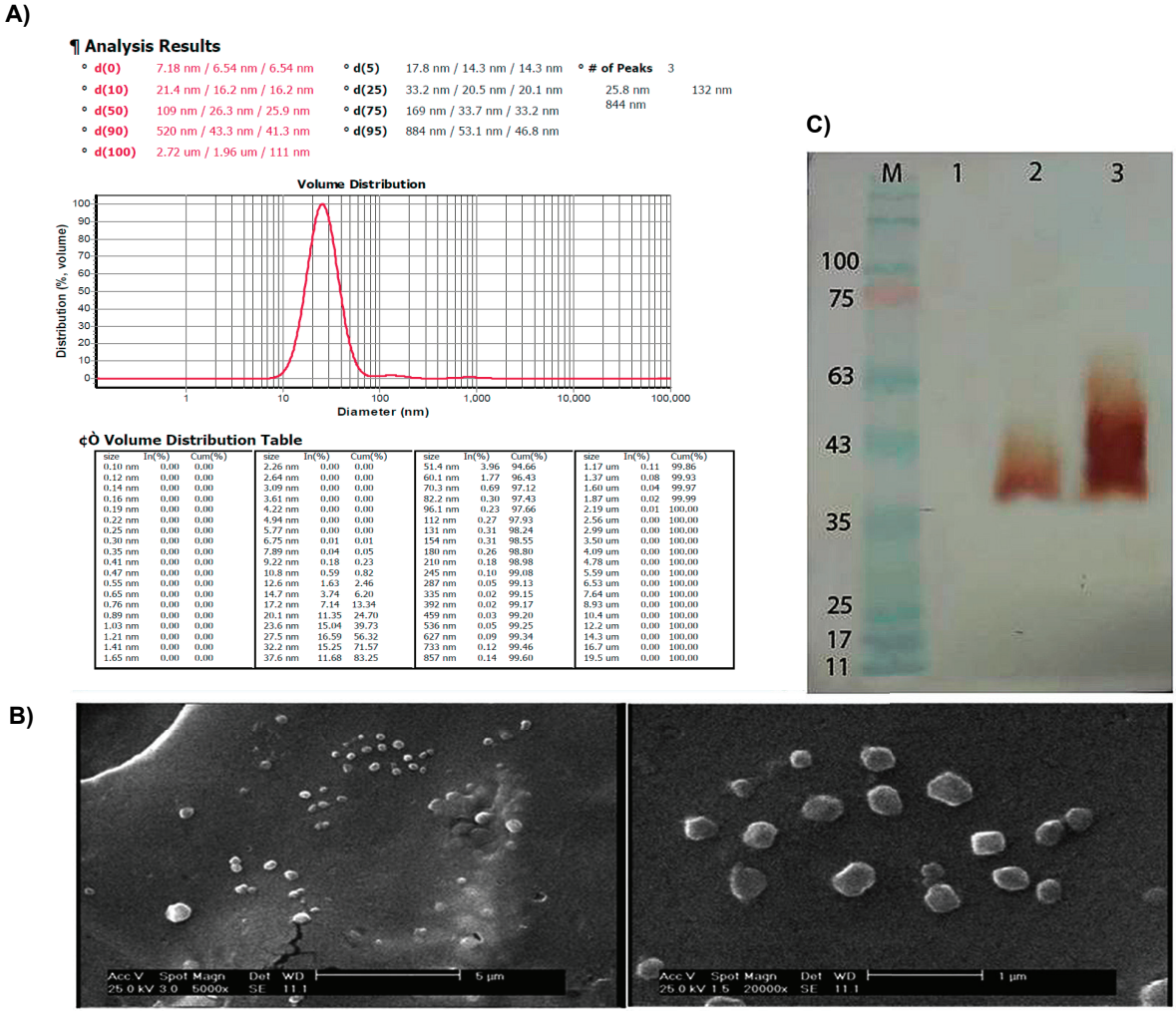

Figure 1. Characterization of adipose mesenchymal stem cell-derived exosomes (AD-MSC-DE). A) The DLS measurement showed the size of AD-MSC-DE. **B**) The SEM images showed the size and shape of AD-MSC-DE. **C**) Western blot analysis for the CD63 (Line 3) isolated exosomes (Line 2) cell lysate. (Line 1) Negative Control, M= Marker.

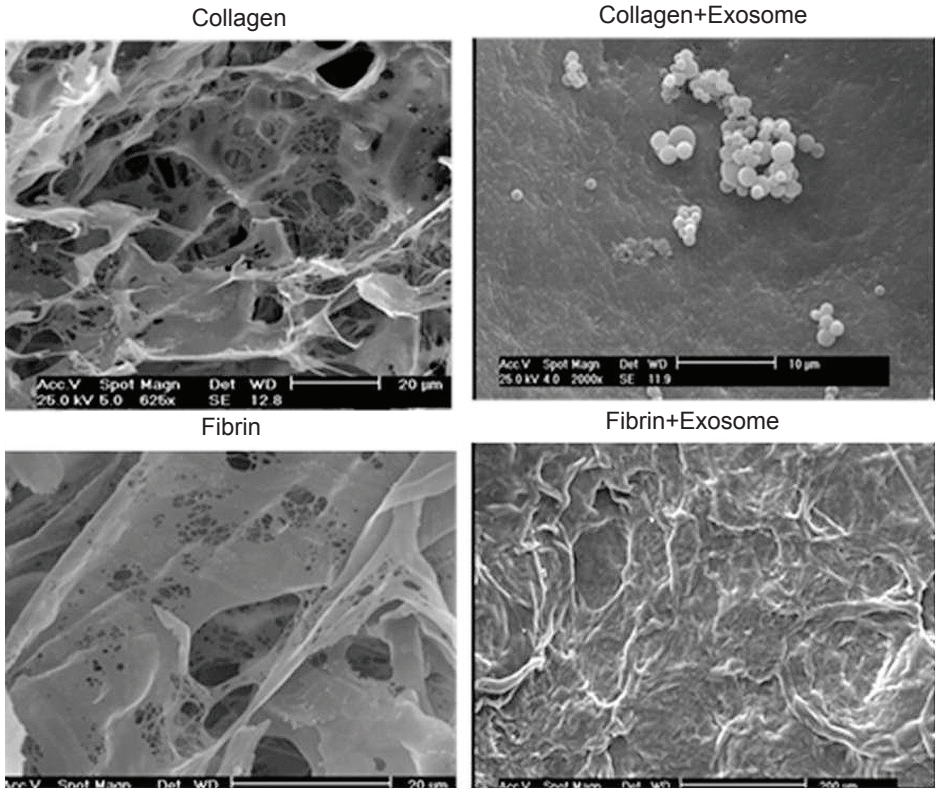

Figure 2. SEM images of AD-MSC-DE in collagen and fibrin hydrogel. A) Scanning electron microscopy of Collagen and Collagen +Exosome hydrogels. **B**) Scanning electron microscopy of Fibrin and Fibrin +Exosome hydrogels.

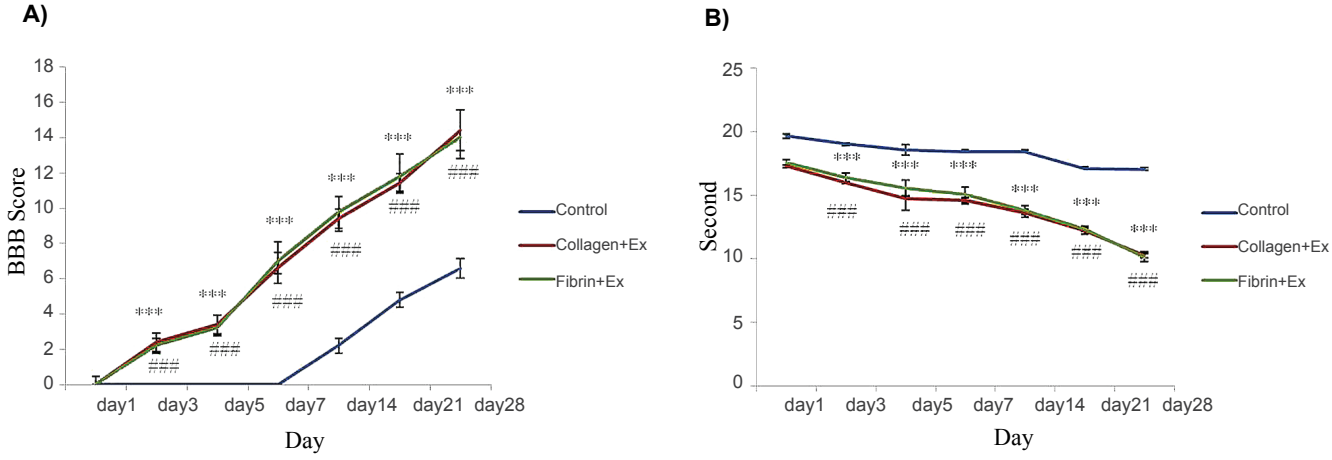

Figure 3. Locomotor scale test (BBB) for assessment of the motor function and thermal scape test for sensory testing. A) The (BBB) Score showed a significant difference between the treatment groups and the control group at days 3,5,7,14 and 28 days post-treatment. ### indicates $P < 0.001$ Vs. the control group, *** indicates $P < 0.001$ Vs. the control group. **B**) Thermal escape testing revealed increased heat sensitivity in the exosome+hydrogel scaffold groups compared to the control groups. ### indicates $P < 0.001$ Vs. the control group, *** indicates $P < 0.001$ Vs. the control group.

4.3. Scanning Electron Microscopy of the Scaffold Containing the Exosomes

The images obtained from SEM of fibrin, collagen, fibrin+exosome, and collagen+exosome are presented in **Figure 2**.

4.4. Animal Study

4.4.1. BBB Scoring

The results obtained from the evaluation of the locomotion performance of SCI rats using BBB scoring are shown in **Figure 3**. Treatment of the rats with both fibrin+ exosome and collagen+ exosome, showed faster functional recovery at all-time points indicated by a gradual upward trend in the BBB score than that of the control group ($p<0.001$) (**Fig. 3A**). There was no significant difference between fibrin+ exosome and collagen+ exosome groups in terms of BBB score ($p>0.05$).

4.4.2. Thermal Sensitivity Test

The results obtained from the evaluation of the thermal sensitivity of SCI rats are shown in **Figure 3B**. Treatment of the rats in the fibrin+exosome and collagen+exosome groups showed a faster positive response within the various times compared to the control group ($p<0.001$) **(Fig. 3B)**. There was no significant difference between fibrin+exosome and collagen+exosome groups in terms of thermal sensitivity ($p>0.5$).

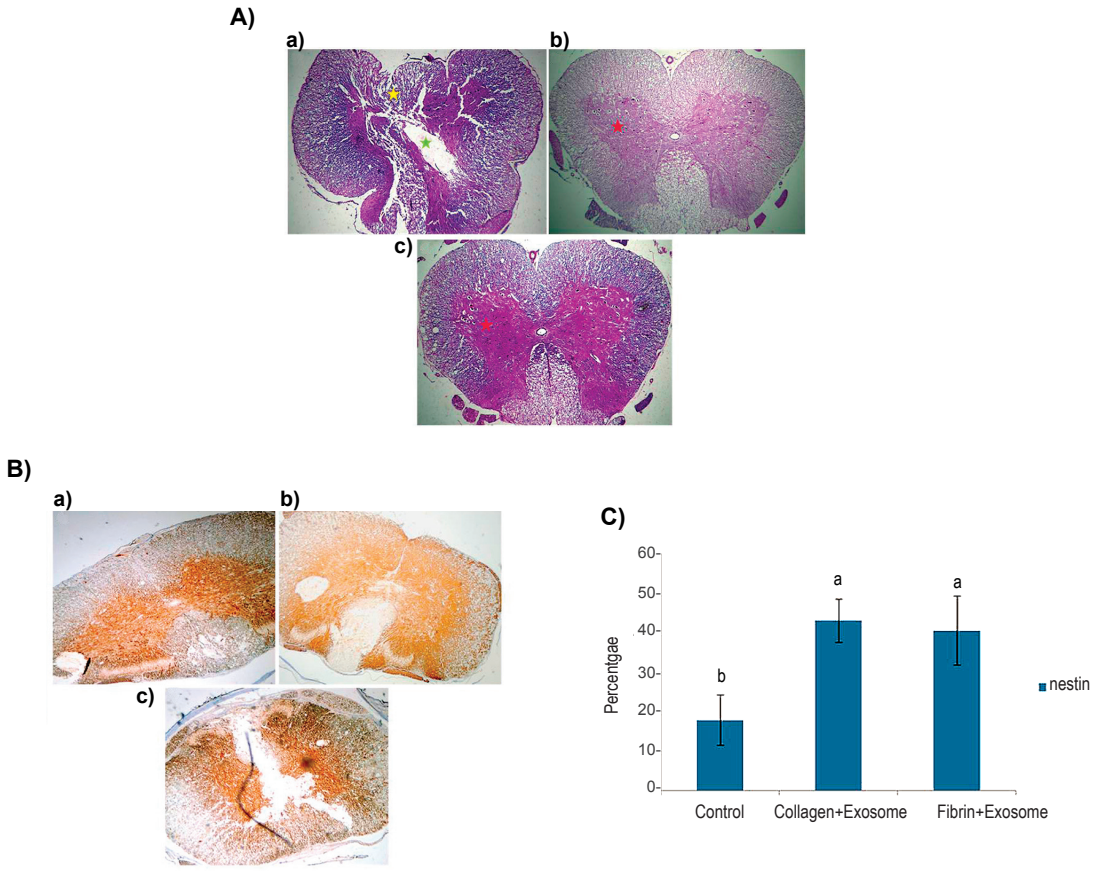

Figure 4. Tissue Staining in Histological Section (H&E, IHC). A) Hematoxylin and eosin staining. a) Disturbance of the white structure (yellow star) and gray matter (green star) of the spinal cord was observed in the control group. **b)** Regeneration of nerve fibers (red stars) has been observed in collagen hydrogen exosome and **c)** fibrin hydrogen + exosome groups. **B) Immunohistological Staining. a)** NF protein expression in the collagen hydrogel + AD-MSC-DE. **b)** NF protein expression in the fibrin hydrogel +AD-MSC-DE. **c)** The control group. **C)** Column graph of statistical analysis of nestin protein expression percentage with ImagJ in different groups, unlike letters indicate differences significance is at $p<0.05$ level.

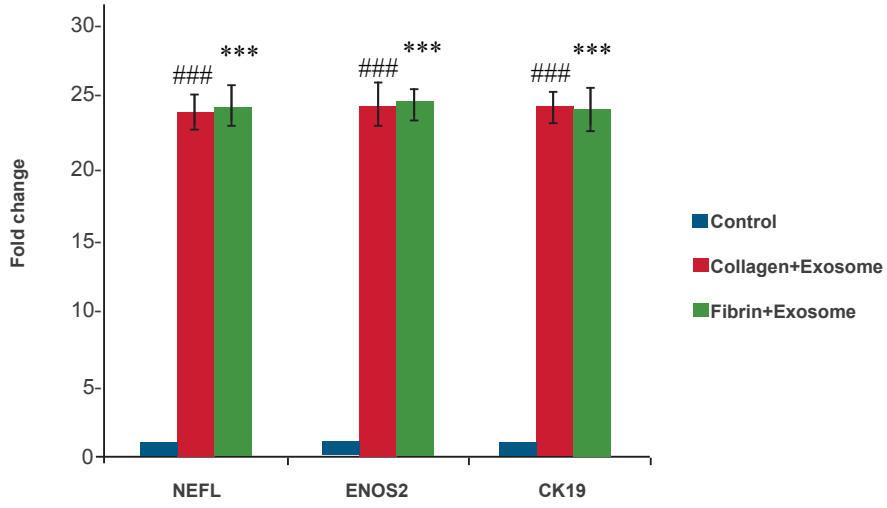

Figure 5. Real Time PCR for NEFL, ENOS and CK19 genes. The mRNA expression level of NEFL, eNOS, and CK19 in the collagen hydrogel+ AD-MSC-DE and fibrin hydrogel +AD-MSC-DE groups. The expression level of NEFL and Enos mRNA in control group were considered as 1, and the others were expressed as folds compared to the control. ### indicates $P < 0.001$ Vs. The control group, *** indicates $P < 0.001$ Vs. the control group

4.4.3. Histopathological and IHC

Histologically, disruption of the white and gray matter of the spinal cord structure defined as severe polio and Leuko-Myelomalacia, respectively, was detected in the control group. The improved histological areas in the injured site indicated the regeneration of nerve fibers was seen in the both collagen hydrogel+exosome and fibrin hydrogel+exosome groups **(Fig. 4A**). The collagen and fibrin hydrogel scaffold+AD-MSC-DE groups equally treated the SCI lesion, histologically.

Immunohistochemically, collagen and fibrin hydrogel scaffold+AD-MSC-DE groups showed considerable NF protein expression compared to the control group (**Fig. 4B**). There was no significant difference between fibrin+exosome and collagen+exosome groups res-pected to NF protein expression (p>0.5).

4.4.4. Molecular Assay

The mean expression levels of NEFL, eNOS, and CK19 mRNA were up-regulated by 23.82, 24.31, and 24.23 fold in the collagen hydrogel+ AD-MSC-DE compared to the control group. The mean expression levels of NEFL, eNOS, and CK19 mRNA were up-regulated by 24.33, 24.53, and 23.98 fold in the fibrin hydrogel+AD-MSC-DE compared to the control group (**Fig. 5**).

There was no significant difference between fibrin+exosome and collagen+exosome groups respected to the mRNA expression levels of NEFL, eNOS, and CK19 (p>0.5). The experiment was done in triplicate.

5. Discussion

SCI is a considerable and serious portion of the global injury burden with a prevalence of 27.04 million in the world that is mostly caused by road accidents and falls (27-30). In this study, the treatment effects of collagen and fibrin hydrogels encapsulated with AD-MSC-DE were demonstrated and compared for the treatment of SCI in a rat animal model using clinical, histological, immunohistochemical, and molecular assays. Exosomes encapsulated in fibrin gel have been recently shown to enhance neurogenesis through over-expressing VGF in the SCI mice model (31). Li *et al*. (2020) demonstrated that the laminin hydrogels and MSC-derived exosomes promote the regeneration of the spinal cord and the recovery of hind-limb motor function after SCI (32). The effect of exosomes derived from stem cells encapsulated within ECM-

based scaffolds has been rarely investigated. However, a comparison of the effects of the exosomes derived from adipose tissue stem cells encapsulated within two ECM-based scaffolds including fibrin and collagen on SCI has yet to be investigated. MSC, as the sources of exosomes, are originally discovered in bone marrow, adipose tissue, the placenta, the umbilical cord, the amniotic membrane, the fetal lung, gingiva, and dental pulp (33, 34). However, the exosomes can be collected from adipose tissue in a non-invasive manner without ethical limitations, unlike the other sources.

In the first step of the study, the AD-MSC-DEs were approved by Western blot, SEM, and DLS. Among the several treatment approaches for treating SCI, the exosomes considered EVs seem to be the most promising (35). To characterize the AD-MSC-DEs, the SEM and DLS measurement as well as the Western blot analysis for the CD63 marker were done. CD63 is a general marker of EVs, however, it can be present in different amounts in EV subpopulations and enriched in EVs derived from different cell lines (36). DLS measurement and SEM analysis showed that the size of the isolated exosomes derived from the AD-MSC is less than 100 nM. Exosomes, the nano-sized exfoliated membranes, are distinguished from other EVs i.e. shedding microvesicles (or ectosomes; 100-1,000 nM) and apoptotic bodies (released during apoptosis; 1-5 μM) based on their size and surface markers (18). The isolated AD-MSC-DEs were cup-shaped in SEM. Explicitly, exosomes are Nano-sized exfoliated membrane vesicles that are defined as extra-cellular vesicles with a diameter of 40–100 nm, and "cup-shaped" morphology when analyzed by SEM (17).

EVs such as exosomes secreted from different MSC, promote the activation of endogenous neural progenitor cells (37), reduce pericyte pyroptosis and increase the survival rate of pericytes, promote the survival rate of neurons as well as the extension of nerve fibers (38), promote angiogenesis (39), reduce tissue damage and cell death, improve neurological recovery (40), down-regulate the expression of inflammatory cytokines and decrease astrogliosis and gliosis scars (41), and attenuate cellular apoptosis and inflammation (42) and finally improve the urinary bladder dysfunction and hind limb locomotor function in an animal model of SCI. Although the induction of inflammatory processes and activated immune cells such as microglia, macrophages, and neutrophils contribute to eliminating the cellular debris at the SCI site, the inflammatory reactions do not resolve and become deleterious chronic processes hindering regeneration. Therefore, the induction of chronic inflammatory responses after SCI is a pivotal initiating event for the course of secondary damages (43-45). In this study, the exosomes were derived from AD-MSC. The effectiveness of MSC to control inflammatory responses by paracrine signaling on immune cells has been widely demonstrated. Additionally, the exosomes secreted by MSC have been recently shown to carry both anti-scarring and inflammatory activities resembling the ones of their parental MSC (41).

Fibrin and collagen hydrogels were used in this study. Collagen is the main ECM component in different natural tissues such as CNS (46). We have recently demonstrated that collagen and fibrin hydrogels encapsulation with MSC have therapeutic effects in rat SCI model (26). Both hydrogels used in this study promote axonal regeneration and repair of SCI by several pathways and mechanisms. Fibrin and collagen hydrogels can reversibly bind to various cytokines of growth factors (GFs) such as vascular endothelial GF (VEGF), fibroblast GF (FGF), platelet-derived GF (PDGF), and neurotrophin-3(NT-3) leading to the repair of SCI and promote motor function recovery (47, 48). In addition, hydrogels provide a permissive environment for M2 macrophages to participate in the regeneration of injury (49). Collagen hydrogel increases oligodendrocyte differentiation of neural progenitor cells that are needed for SCI treatment (50). Two primary and secondary injuries are contributed to the pathologic process of SCI (51). The hydrogels carrying erythropoietin have been shown to promote nerve regeneration and motor function recovery in the regeneration of the early phase of compression injury (52).

For clinical evaluation BBB scorning system and thermal escape test were used. Treatment of the rats with fibrin+AD-MSCs-DE and collagen+AD-MSCs-DE showed faster functional recovery at all-time points indicated by a gradual upward trend in the BBB score than that of the control group. In addition, escape testing following treatment and sham groups revealed increased heat sensitivity in the fibrin+ AD-MSC-DE and collagen+AD-MSCs-DE groups compared to the control groups. This finding showed that could improve

nerve injury-induced neuropathic pain. The thermal escape test is a technique that can be used to further characterize the recovery of SCI dogs (53). Nerve injury-induced neuropathic pain and SCI-induced allodynia are difficult to treat. The exosomes derived from MSC have been previously used for the treatment of nerve injury-induced pain in rats (54). Within a few days after SCI, heat, and cold super-sensitivity appeared at the lesion site (55).

The data obtained from the expression level of NEFL, eNOS2, CK19, and IVL in rat SCI models showed that the NEFL, eNOS2, CK19, and IVL are expressed at high levels in the injured spinal cord tissue and treated with fibrin and collagen hydrogels encapsulated with AD-MSC-DE. NEFL plays an important role in axonal transport and nerve conduction velocity by encoding a neuronal protein that is vital for neurofilament formation (56). NEFL has been recently shown to be the first expressed neurofilament gene in the path of axonal regeneration in SCI (57). Although alterations in eNOS expression induced by injury are more variable, eNOS is not normally expressed in SCI tissue (58, 59). CK-19 was up-regulated in the treatment groups compared to the control group. CK-19 is closely related to endometrial proliferation and differentiation involved in angiogenesis (37).

6. Conclusion

This study was designed to investigate a new combined, synergic, efficient, and suitable method for the treatment of the rat SCI model. Exosomes combined with both hydrogels are more effective compared to AD-MSC with both hydrogels in the treatment of rat SCI model. The extracted exosome from Adipose tissue is a safe and reliable source for SCI treatment in parallel with AD- MSC in both hydrogels. There is no difference between the 2 types of hydrogel for the treatment of the rat SCI model. Further investigations are required to administrate exosomes as a cell-derived product in preclinical or human clinical trial.

Data Availability

The datasets used and/or analyzed during the current study are available from the corresponding author upon reasonable request.

Acknowledgments

Not applicable

Statements and Declarations

Funding None.

Competing Interests

The authors have no financial interest.

Author's Contributions

Jafar Ai designed the study. All authors contributed to data collecting. The first draft of the manuscript was prepared by Zohreh Afsartala and Sadegh Shirian. All authors read and approved the final manuscript.

Ethical approve

The study was approved by the Ethical Committee of TUMS (Ethical No: IR.TUMS.VCR.REC.13980.684).

Consent to participate

Not applicable.

Consent to publish

Not applicable.

References

1. James SL, Theadom A, Ellenbogen RG, Bannick MS, Montjoy-Venning W, Lucchesi LR, Abbasi N, Abdulkader R, Abraha HN, Adsuar JC, Afarideh M. Global, regional, and national burden of traumatic brain injury and spinal cord injury, 1990–2016: a systematic analysis for the Global Burden of Disease Study 2016. *Lancet Neurol*. 2019;**18**(1):56-87. doi:10.1016/S0140-6736(17)32154-2
2. Rubiano AM, Carney N, Chesnut R, Puyana JC. Global neurotrauma research challenges and opportunities. *Nature*. 2015;**527**(7578):S193-S197. doi: 10.1038/nature16035.
3. Fakhoury M. Spinal cord injury: overview of experimental approaches used to restore locomotor activity. *Rev Neurosci*. 2015;**26**(4):397-405. doi: 10.1515/revneuro-2015-0001.
4. Liu WZ, Ma ZJ, Li JR, Kang XW. Mesenchymal stem cell-derived exosomes: therapeutic opportunities and challenges for spinal cord injury. *Stem Cell Res Ther*. 2021;**12**:102. doi: 10.1186/s13287-021-02153-8.
5. Hawryluk G, Whetstone W, Saigal R, Ferguson A, Talbott J, Bresnahan J, Dhall S, Pan J, Beattie M, Manley G. Mean arterial blood pressure correlates with neurological recovery after human spinal cord injury: analysis of high frequency physiologic data. *J Neurotrauma*. 2015; **32**(24):1958-1967. doi: 10.1089/neu.2014.3778.
6. Fehlings MG, Vaccaro A, Wilson JR, Singh A, W. Cadotte D, Harrop JS, Aarabi B, Shaffrey C, Dvorak M, Fisher C, Arnold P. Early versus delayed decompression for traumatic cervical spinal cord injury: results of the Surgical Timing in Acute Spinal Cord Injury Study (STASCIS). *PloS One*. 2012;**7**(2):e32037. doi: 10.1371/journal.pone.0032037.
7. Mahya S, Ai J, Shojae S, Khonakdar HA, Darbemamieh G, Shirian S. Berberine loaded chitosan nanoparticles encapsulated in polysaccharide-based hydrogel for the repair of spinal cord. *Int J Biol Macromol*.2021;**182**:82-90. doi:

10.1016/j.ijbiomac.2021.03.106.
8. Squair JW, DeVeau KM, Harman KA, Poormasjedi-Meibod MS, Hayes B, Liu J, Magnuson DS, Krassioukov AV, West CR. Spinal cord injury causes systolic dysfunction and cardiomyocyte atrophy. *J Neurotrauma*. 2018;**35**(3):424-434. doi: 10.1089/neu.2017.4984.
9. Wutte C, Klein B, Becker J, Mach O, Panzer S, Strowitzki M, Maier D, Grassner L. Earlier decompression (< 8 hours) results in better neurological and functional outcome after traumatic thoracolumbar spinal cord injury. *J Neurotrauma* 2019;**36**(12):2020–2027. doi: 10.1089/neu.2018.6146.
10. Streijger F, So K, Manouchehri N, Gheorghe A, Okon EB, Chan RM, Ng B, Shortt K, Sekhon MS, Griesdale DE, *et al*. A direct comparison between norepinephrine and phenylephrine for augmenting spinal cord perfusion in a porcine model of spinal cord injury. *J Neurotrauma*. 2018;**35**(12):1345-1357. doi: 10.1089/neu.2017.5285.
11. Tran AP, Warren PM, Silver J. The biology of regeneration failure and success after spinal cord injury. *Physiologic Rev* 2018;**98**(2):881-917. doi: 10.1152/physrev.00017.2017.
12. Li L, Xiao B, Mu J, Zhang Y, Zhang C, Cao H, Chen R, Patra HK, Yang B, Feng S, Tabata Y. Spinal Cord Repair via Regulating Reactive Oxygen Species Microenvironment and Synergizing with Mesenchymal Stem Cells. *ACS Nano* 2019;**13**;14283–14293. doi: 10.1021/acsnano.9b07598.
13. Ronaghi M, Erceg S, Moreno-Manzano V, Stojkovic M. Challenges of stem cell therapy for spinal cord injury: human embryonic stem cells, endogenous neural stem cells, or induced pluripotent stem cells? *Stem Cells*. 2010;**28**(1):93-99. doi: 10.1002/stem.253.
14. Assinck P, Duncan GJ, Hilton BJ, Plemel JR, Tetzlaff W. Cell transplantation therapy for spinal cord injury. *Nature Neurosci*. 2017;**20**(5):637-647. doi: 10.1038/nn.4541.
15. Bakhtiarimoghadam B, Shirian S, Mirzaei E, Sharifi S, Karimi I, Gharati G, Takallu S, Nazari H. Comparison capacity of collagen hydrogel, mix-powder and in situ hydroxyapatite/ collagen hydrogelscaffolds with and without mesenchymal stem cells and platelet-rich plasma in regeneration of critical sized bone defect in a rabbit animal model. *J Biomed Mater Res Part B: Applied Biomaterials*. 2021;**109**(12):2199-2212. doi: 10.1002/jbm.b.34867.
16. Gharati G, Shirian S, Sharifi S, Mirzaei E, Bakhtirimoghadam B, Karimi I, Nazari H. Comparison Capacity of Collagen Hydrogel and Collagen/Strontium Bioglass Nanocomposite Scaffolds with and Without Mesenchymal Stem Cells in Regeneration of Critical Sized Bone Defect in a Rabbit Animal Model. *Biol Trace Elem Res*. 2022;**200**(7):3176-3186. doi: 10.1007/s12011-021-02909-6.
17. Liu SL, Sun P, Li Y, Liu SS, Lu Y. Exosomes as critical mediators of cell-to-cell communication in cancer pathogenesis and their potential clinical application. *Transl Cancer Res*. 2019;**8**:298-311. doi: 10.21037/tcr.2019.01.03.
18. Norouzi-Barough L, Shirian S, Gorji A, Sadeghi M. Therapeutic potential of mesenchymal stem cell-derived exosomes as a cell-free therapy approach for the treatment of skin, bone, and cartilage defects. *Conn Tissue Res*. 2022;**63**(2):83-96. doi: 10.1080/03008207.2021.1887855.
19. Norouzi-Barough L, Asgari Khosroshahi A, Gorji A, Zafari F, Shahverdi Shahraki M, Shirian S. COVID-19-Induced Stroke and the Potential of Using Mesenchymal Stem Cells-Derived Extracellular Vesicles in the Regulation of Neuroinflammation. *Cell Mol Neurobiol*.2022;**13**:1-10. doi: 10.1007/s10571-021-01169-1.
20. Shi Q, Qian Z, Liu D, Sun J, Wang X, Liu H, Xu J, Guo X. GMSC-Derived Exosomes Combined with a Chitosan/Silk Hydrogel Sponge Accelerates Wound Healing in a Diabetic Rat Skin Defect Model. *Front Physiol* 2017;**8**:904. doi: 10.3389/ fphys.2017.00904.
21. Ebrahimi-Barough S, Norouzi Javidan A, Saberi H, Joghataei MT, Rahbarghazi R, Mirzaei E, Faghihi F, Shirian S, Ai A, Ai J. Evaluation of Motor Neuron-Like Cell Differentiation of hEnSCs on Biodegradable PLGA Nanofiber Scaffolds. *Mol Neurobiol*. 2015;**52**(3):1704-1713. doi: 10.1007/s12035-014-8931-2.
22. Kielkopf CL, Bauer W, Urbatsch IL. Bradford Assay for Determining Protein Concentration. *Cold Spring Harb Protoc*. 2020;**2020**(4):102269. doi: 10.1101/pdb.prot102269.
23. Lyu TS, Ahn Y, Im YJ, Kim SS, Lee KH, Kim J, Choi Y, Lee D, Kang E, Jin G, Hwang J. The characterization of exosomes from fibrosarcoma cell and the useful usage of Dynamic Light Scattering (DLS) for their evaluation. *Plos One*. 2021;**16**(1):e0231994. doi: 10.1371/journal.pone.0231994.
24. Abdolahi S, Aligholi H, Khodakaram-Tafti A, Khaleghi Ghadiri M, Stummer W, Gorji A. Improvement of rat spinal cord injury following lentiviral vector-transduced neural stem/ progenitor cells derived from human epileptic brain tissue transplantation with a self-assembling peptide scaffold. *Mol Neurobiol*. 2021;**58**(6):2481-2493. doi: 10.1007/s12035-020-02279-5.
25. Memary E, Imani A, Arhamidolatabadi A, Fadavi P, Aghajani M, Mohebzadeh F, Shahverdi-Shahraki M, Dabbagh A, Mirkheshti A, Shirian S. The Neuroprotective Effects of Administration of Methylprednisolone in Cardiopulmonary Resuscitation in Experimental Cardiac Arrest Model. *Cell Mol Neurobiol*. 2022:1-13. doi: 10.1007/s10571-022-01300-w.
26. Afsartala Z, Hajighasem M, Shirian S. Comparison of the Regenerative Effect of Adipose Tissue Mesenchymal Stem Cell Encapsulated into Two Hydrogel Scaffolds on Spinal Cord Injury. *Arch Neurosci.*2022;9:1. doi: 10.5812/ ans.119170
27. WagnerF, Mignardot J, Le Goff-Mignardot C, Demesmaeker R, Komi S, Capogrosso M, *et al*. Targeted neurotechnology restores walking in humans with spinal cord injury. *Nature* .2018;**563**:65-71. doi: 10.1038/s41586-018-0649-2.
28. David G, Mohammadi S, Martin A, Cohen-Adad J, Weiskopf N, Thompson A, *et al*. Traumatic and nontraumatic spinal cord injury: pathological insights from neuroimaging. *Nat Rev Neurol.* 2019;**15**:718-731. doi: 10.1038/s41582-019-0270-5
29. Hutson T, Di Giovanni S. The translational landscape in spinal cord injury: focus on neuroplastcity and regeneration. *Nat Rev Neurol.* 2019;**15**:732-745. doi: 10.1038/s41582-019-0280-3
30. Ordikhani F, Sheth S, Zustiak S. Polymeric particle-mediated molecular therapies to treat spinal cord injury. *Int J Pharm. (Amsterdam Neth.)* .2017;**516**(1-2):71-81. doi: 10.1016/j. ijpharm.2016.11.021
31. He X, Yang L, Dong K.*et al*. Biocompatible exosome-modified fibrin gel accelerates the recovery of spinal cord injury by VGF-mediated oligodendrogenesis. *J Nanobiotechnol.*2022;**20**:360. doi: 10.1186/s12951-022-01541-3
32. Li L, Zhang Y, Mu J, Chen J, Zhang C, Cao H, Gao J. Transplantation of human mesenchymal stem-cell-derived

exosomes immobilized in an adhesive hydrogel for effective treatment of spinal cord injury. *Nano Lett*.2020;**20**(6):4298-4305. doi: 10.1021/acs.nanolett.0c00929.

33. Zhang X, Huang F, Li W, Dang JL, Yuan J, Wang J, Zeng DL, Sun CX, Liu YY, Ao Q, Tan H. Human gingiva-derived mesenchymal stem cells modulate monocytes/macrophages and alleviate atherosclerosis. *Front Immunol*. 2018;**30**;9:878. doi: 10.3389/fimmu.2018.00878.
34. Zhang Y, Xu J, Liu S, Lim M, Zhao S, Cui K, Zhang K, Wang L, Ji Q, Han Z, Kong D. Embryonic stem cell-derived extracellular vesicles enhance the therapeutic effect of mesenchymal stem cells. *Theranostics*. 2019;**9**(23):6976. doi: 10.7150/thno.35305.
35. Jia Y, Yang J, Lu T, Pu X, Chen Q, Ji L, Luo C. Repair of spinal cord injury in rats via exosomes from bone mesenchymal stem cells requires sonic hedgehog. *Regen Ther*.2021;**18**:309-315. doi: 10.1016/j.reth.2021.08.007
36. Campos-Silva C, Suárez H, Jara-Acevedo R, Linares-Espinós E, Martinez-Piñeiro L, Yáñez-Mó M, Valés-Gómez M. High sensitivity detection of extracellular vesicles immune-captured from urine by conventional flow cytometry. *Sci Rep*. 2019;**9**(1):2042. doi: 10.1038/s41598-019-38516-8.
37. Zhou W, Silva M, Feng, C. *et al.* Exosomes derived from human placental mesenchymal stem cells enhanced the recovery of spinal cord injury by activating endogenous neurogenesis. *Stem Cell Res Ther*. 2021;**12**:174. doi: 10.1186/s13287-021-02248-2.
38. Zhou Y, Wen LL, Li YF, Wu KM, Duan RR, Yao YB, Jing LJ, Gong Z, Teng JF, Jia YJ. Exosomes derived from bone marrow mesenchymal stem cells protect the injured spinal cord by inhibiting pericyte pyroptosis. *Neural Regen Res*. 2022;**17**(1):194-202. doi: 10.4103/1673-5374.314323.
39. Zhong D, Cao Y, Li CJ, Li M, Rong ZJ, Jiang L, Guo Z, Lu HB, Hu JZ. Neural stem cell-derived exosomes facilitate spinal cord functional recovery after injury by promoting angiogenesis. *Exp Biol Med* (Maywood). 2020;**245**(1):54-65. doi: 10.1177/1535370219895491.
40. Huang JH, Fu CH, Xu Y, Yin XM, Cao Y, Lin FY. Extracellular vesicles derived from epidural fat-mesenchymal stem cells attenuate NLRP3 inflammasome activation and improve functional recovery after spinal cord injury. *Neurochem Res*. 2020;**45**(4):760-771. doi: 10.1007/s11064-019-02950-x.
41. Romanelli P, Bieler L, Scharler C, Pachler K, Kreutzer C, Zaunmair P, Jakubecova D, Mrowetz H, Benedetti B, Rivera FJ, Aigner L. Extracellular vesicles can deliver anti-inflammatory and anti-scarring activities of mesenchymal stromal cells after spinal cord injury. *Front Neurol*. 2019;**10**:1225. doi: 10.3389/fneur.2019.01225.
42. Huang JH, Yin XM, Xu Y, Xu CC, Lin X, Ye FB, Cao Y, Lin FY. Systemic administration of exosomes released from mesenchymal stromal cells attenuates apoptosis, inflammation, and promotes angiogenesis after spinal cord injury in rats. *J Neurotrauma*. 2017;**34**(24):3388-3396. doi: 10.1089/neu.2017.5063.
43. Biglari B, Swing T, Child C, Büchler A, Westhauser F, Bruckner T, *et al*. A pilot study on temporal changes in IL-1β and TNF-α serum levels after spinal cord injury: the serum level of TNF-α in acute SCI patients as a possible marker for neurological remission. *Spinal Cord*.2015;**53**:510-514. doi: 10.1038/sc.2015.28.
44. Greenhalgh AD, David S. Differences in the phagocytic response of microglia and peripheral macrophages after spinal cord injury and its effects on cell death. *J Neurosci*.2014;**34**:6316-6322. doi: 10.1523/JNEUROSCI.4912-13.2014.
45. Dibaj P, Nadrigny F, Steffens H, Scheller A, Hirrlinger J, Schomburg ED, *et al*. NO mediates microglial response to acute spinal cord injury under ATP control *in vivo*. *Glia.* 2010 **58**:1133-1144. doi: 10.1002/glia.20993.
46. Chen C, Zhao ML, Zhang RK, Lu G, Zhao CY, Fu F, Sun HT, Zhang S, Tu Y, Li XH. Collagen/heparin sulfate scaffolds fabricated by a 3D bioprinter improved mechanical properties and neurological function after spinal cord injury in rats. *J Biomed Mater Res A*. 2017;**105**(5):1324-1332. doi: 10.1002/jbm.a.36011.
47. Yu Z, Li H, Xia P, Kong W, Chang Y, Fu C, Wang K, Yang X, Qi Z. Application of fibrin-based hydrogels for nerve protection and regeneration after spinal cord injury. *J Biol Eng*. 2020;**14**:22. doi: 10.1186/s13036-020-00244-3
48. Johnson PJ, Tatara A, Shiu A, Sakiyama-Elbert SE. Controlled release of Neurotrophin-3 and platelet-derived growth factor from fibrin scaffolds containing neural progenitor cells enhances survival and differentiation into neurons in a subacute model of SCI. *Cell Transplant*. 2010;**19**(1):89-101. doi: 10.3727/096368909X477273.
49. Chiu C-W, Huang W-H, Kuo H-S, Tsai M-J, Chen C-J, Lee M-J, *et al*. Local inhibition of matrix metalloproteinases reduced M2 macrophage activity and impeded recovery in spinal cord transected rats after treatment with fibroblast growth factor-1 and nerve grafts. *Neural Regen Res*. 2018;**13**(8):1447-1454. doi: 10.4103/1673-5374.235302
50. Geissler SA, Sabin AL, Besser RR, Gooden OM, Shirk BD, Nguyen QM, Khaing ZZ, Schmidt CE. Biomimetic hydrogels direct spinal progenitor cell differentiation and promote functional recovery after spinal cord injury. *J Neural Eng*. 2018;**15**(2):025004. doi: 10.1088/1741-2552/aaa55c.
51. Javdani M, Habibi A, Shirian S, Kojouri GA, Hosseini F. Effect of selenium nanoparticle supplementation on tissue inflammation, blood cell count, and IGF-1 levels in spinal cord injury-induced rats. *Biol Trace Elem Res.* 2019;**187**(1):202-211. doi: 10.1007/s12011-018-1371-5.
52. Sundem L, Tseng K-CC, Li H, Ketz J, Noble M, Elfar J. Erythropoietin enhanced recovery after traumatic nerve injury: myelination and localized effects. *J Hand Surg Am*. 2016;**41**(10):999-1010. doi: 10.1016/j.jhsa.2016.08.002
53. Gorney AM, Blau SR, Dohse CS, Griffith EH, Williams KD, Lim JH, Knazovicky D, Lascelles BD, Olby NJ. Mechanical and thermal sensory testing in normal chondrodystrophoid dogs and dogs with spinal cord injury caused by thoracolumbar intervertebral disc herniations. *J Vet Intern Med*. 2016;**30**(2):627-635. doi: 10.1111/jvim.13913.
54. Shiue SJ, Rau RH, Shiue HS, Hung YW, Li ZX, Yang KD, Cheng JK. Mesenchymal stem cell exosomes as a cell-free therapy for nerve injury-induced pain in rats. *Pain*. 2019;**160**(1):210-223. doi: 10.1097/j.pain.0000000000001395
55. Hoschouer EL, Basso DM, Jakeman LB. Aberrant sensory responses are dependent on lesion severity after spinal cord contusion injury in mice. *Pain* 2010;**148**:328-342. doi: 10.1016/j.pain.2009.11.023.
56. Yang Y, Gu LQ, Burnette WB, Li J. N98S mutation in NEFL gene is dominantly inherited with a phenotype of polyneuropathy and cerebellar atrophy. *J Neurol Sci.* 2016;**365**:46-47. doi: 10.1016/j.jns.2016.04.007.

57. Valeri A, Chiricosta L, Gugliandolo A, Pollastro F, Mazzon E. Will Cannabigerol Trigger Neuroregeneration after a Spinal Cord Injury? An *in Vitro* Answer from NSC-34 Scratch-Injured Cells Transcriptome. *Pharmaceuticals*. 2022;**15**(2):117. doi: 10.3390/ph15020117.
58. Yang JY, Kim, HS, Lee JK. Changes in nitric oxide synthase expression in young and adult rats after spinal cord injury. *Spinal Cord*.2007;**45**:731-738. doi: 10.1038/sj.sc.3102036.
59. Zhang L, Li Y, Guan CY. *et al.* Therapeutic effect of human umbilical cord-derived mesenchymal stem cells on injured rat endometrium during its chronic phase. *Stem Cell Res Ther.* 2018;**9**:36. doi: 10.1186/s13287-018-0777-5.